

Theoretical aspects of image formation in the aberration-corrected electron microscope

H. Rose

Institute of Applied Physics, TU Darmstadt, Hochschulstrasse 6, 64289 Darmstadt, Germany

ARTICLE INFO

Dedicated to Professor Dr. Hannes Lichte on the occasion of his 65th birthday

Keywords:

Image formation
Damping envelope
Bright-field contrast
Obstruction-free phase shifter

ABSTRACT

The theoretical aspects of image formation in the transmission electron microscope (TEM) are outlined and revisited in detail by taking into account the elastic and inelastic scattering. In particular, the connection between the exit wave and the scattering amplitude is formulated for non-isoplanatic conditions. Different imaging modes are investigated by utilizing the scattering amplitude and employing the generalized optical theorem. A novel obstruction-free anamorphic phase shifter is proposed which enables one to shift the phase of the scattered wave by an arbitrary amount over a large range of spatial frequencies. In the optimum case, the phase of the scattered wave and the introduced phase shift add up to $-\pi/2$ giving negative contrast. We obtain these optimum imaging conditions by employing an aberration-corrected electron microscope operating at voltages below the knock-on threshold for atom displacement and by shifting optimally the phase of the scattered electron wave. The optimum phase shift is achieved by adjusting appropriately the constant phase shift of the phase plate and the phase shift resulting from the defocus and the spherical aberration of the corrected objective lens. The realization of this imaging mode is the aim of the SALVE project (Sub-Å Low-Voltage Electron microscope).

© 2009 Elsevier B.V. All rights reserved.

1. Introduction

In 1948, Gabor proposed wave-front reconstruction by means of holography as a possibility to eliminate a posteriori the effect of the spherical aberration in electron micrographs by light optical means [1]. However, his envisioned aim to improve the resolution of the electron microscope had not been successful at that time. The main reasons were that a sufficiently coherent quasi-monochromatic electron source did not exist and that the reconstruction of the Gabor inline hologram suffers from the inseparability of the twin images. The latter problem was solved in 1962 by Leith and Upatnicks [2] who introduced a novel type of light-optical hologram known as offset-reference hologram or off-axis hologram, respectively. The reference wave is produced by a prism which is placed in the upper half of the incident plane wave while the lower half propagates through the transparent object. The hologram is taken at a plane where the transmitted wave and the reference wave superpose. In order to employ this technique to electron waves, an equivalent electron-optical prism must be employed. Already in 1956 Moellenstedt and Dueker had solved this problem by introducing the electron-optical biprism consisting of a positively charged wire centered between two parallel plane electrodes [3]. The development of the field emission

electron gun provided the appropriate highly coherent source enabling high-resolution electron holography. Using these instrumental developments, Hannes Lichte established electron holography as an indispensable tool for determining the amplitude and the phase of the electron wave [4,5]. For example, this technique has become an important method for investigating electric and magnetic fields in solid objects on an atomic scale [6].

In accordance with Gabor, we may consider the image taken in a transmission electron microscope (TEM) with parallel illumination as a Fraunhofer inline hologram [7,8]. The information content of this hologram is limited by the incoherent aberrations preventing the transfer of spatial frequencies which are larger than the so-called information limit. In a standard TEM, the instrumental resolution is limited by the unavoidable spherical aberration of the objective lens [9]. Nevertheless, Scherzer showed that this aberration can be utilized together with an appropriately chosen defocus to form a phase plate which shifts the phase of the scattered wave by about $-\pi/2$ for aperture angles θ in the region $\theta_{\min} = 0.3(\lambda/C_3)^{1/4} \leq \theta \leq 1.5(\lambda/C_3)^{1/4} = \theta_{\max}$ [10]. Here λ is the wavelength of the incident electrons, and C_3 denotes the coefficient of the third-order spherical aberration. The relation shows that the phase is only shifted appreciably for spatial frequencies $q = \theta/\lambda$ in the range $q_{\max}/q_{\min} = \theta_{\max}/\theta_{\min} \approx 5$. Spatial frequencies lower than $q_{\min} \approx 0.3(\lambda^3/C_3)^{-1/4}$ do not contribute to the phase contrast. Therefore, structures larger than $1/q_{\min}$ remain invisible in the image of phase objects. To visualize as many

E-mail address: harald.rose@physik.tu-darmstadt.de

structures as possible, ratios $q_{\max}/q_{\min} \geq 100$ are desirable, especially in the case of non-crystalline objects.

The successful correction of spherical aberration and off-axial coma has largely improved the performance of the electron microscope [11,12] and of electron holography [13]. The main advantages are that tilt of illumination does not induce axial coma and that the point spread function is very small. The resulting elimination of delocalization effects enables (a) artifact-free imaging of non-periodic object details such as interfaces and (b) a more accurate determination of the residual phase shift $\chi(\vec{\theta})$ of the corrected objective lens. The precise knowledge of this phase is necessary for an accurate reconstruction of the exit wave by means of holography.

In order to fully understand the formation of the image in the electron microscope or that of an electron hologram, we need a complete quantum mechanical description. Although several theoretical investigations on non-linear imaging theory have been performed in the past [14–16], we revisit this theory in more detail by incorporating some new results. We also demonstrate the connection between the descriptions starting either from the scattering amplitude or from the wave at the exit plane located behind the object. In the ideal case, this plane is perfectly imaged into the Gaussian image plane.

2. Chromatic damping envelope revisited

The chromatic aberration of the objective lens suppresses the transfer of high spatial frequencies in the electron microscope. In the case of phase contrast one considers this effect by multiplying the monochromatic phase contrast transfer function by a Gaussian chromatic damping envelope. One obtains this result mathematically by assuming that the distribution function of the energy spread is Gaussian. This general assumption is unrealistic because the tail of the energy distribution function of any source decreases exponentially with the energy, as it is the case for the Maxwell distribution. However, the Gaussian approximation is well suited to describe the energy distribution of the electrons behind a dispersion-free monochromator, which reduces the energy width of the beam by means of a slit aperture located at the dispersion plane within the monochromator. In order to describe analytically the energy distribution of realistic electron sources without monochromator, we employ the generalized Maxwell distribution

$$g(E) = \frac{(E/b)^n}{\Gamma(n+1)b} e^{-E/b}, \quad n \geq 0, \quad \int_0^{\infty} g(E) dE = 1. \quad (1)$$

Here E is the starting energy of the electron, and

$$\Gamma(n+1) = \int_0^{\infty} x^n e^{-x} dx \quad (2)$$

defines the gamma function. In the case of thermionic electron emission, we have $n=1/2$. The parameter b is connected with the mean emission energy $\langle E \rangle$ and the standard deviation ΔE via the relations

$$\langle E \rangle = \int_0^{\infty} E g(E) dE = b(n+1), \quad \Delta E = (\langle E^2 \rangle - \langle E \rangle^2)^{1/2} = b\sqrt{n+1}. \quad (3)$$

In accordance with the standard assumption we suppose an incoherent effective source. Because no fixed phase relations exist between waves emitted from different points of the effective source, partial incident plane waves with different angles of incidence $\vec{\theta}$ in front of the object are incoherent with each other because they originate from different points of the effective source.

3. Exit wave and scattering amplitude

The wave $\psi_e = \psi(z_e, \vec{\rho}_e, \vec{\theta})$ at the exit plane z_e of the object is a function of the angle of incidence and the lateral distance $\vec{\rho}_e = x_e \vec{e}_x + y_e \vec{e}_y$. In the presence of macroscopic electromagnetic fields in the region behind the exit plane, we must employ the modified Sommerfeld diffraction formula [17]. The elementary wave originating from a point at the exit plane has the asymptotic form

$$P(\vec{r}, \vec{\rho}_e) = a e^{iS(\vec{r}, \vec{\rho}_e)/\hbar} \quad (4)$$

at the point \vec{r} if its distance $z - z_e$ from the exit plane is much larger than the diameter of the illuminated object area. The point eikonal

$$S(\vec{\rho}, \vec{\rho}_e) = \int_{\vec{\rho}_e}^{\vec{r}} \vec{p} d\vec{r} \quad (5)$$

is identical with the path integral taken over the canonical momentum $\vec{p} = \hbar \vec{k} = m \vec{v} + e \vec{A}$ along the classical path of the electron, which connects the starting point at the exit plane with the point of observation $\vec{r} = z \vec{e}_z + \vec{\rho}$. The amplitude of the propagator (4) represents the curvature of the elementary wave. For the field-free space the eikonal and the amplitude adopt the simple forms

$$S = \hbar k |\vec{r} - \vec{r}_e|, \quad a = \frac{1}{|\vec{r} - \vec{r}_e|} \quad (6)$$

In this case, the propagator is a spherical wave emanating from the point $\vec{\rho}_e$ at the exit plane z_e . The semi-classical approximation (4) of the propagator is valid for macroscopic fields as long as the point of observation is not located on the caustic formed by the intersection points of trajectories starting from a single point within a continuous set of differential solid angles. For example, the approximation holds true at the back-focal plane of the objective lens with focal length f_o . At this plane we have

$$a \approx \frac{1}{f_o}, \quad \vec{\rho}/f_o \approx \vec{\theta}, \quad S/\hbar = k(z_f - z_e) - k \vec{\theta} \cdot \vec{\rho}_e - \chi(\vec{\theta}, \vec{\rho}_e, E). \quad (7)$$

In the most general case, the phase shift

$$\chi(\vec{\theta}, \vec{\rho}_e, E) = \chi_g(\vec{\theta}) + \chi_c(\vec{\theta}, E) + \chi_f(\vec{\theta}, \vec{\rho}_e, E) \quad (8)$$

is composed of three terms, the geometrical axial term $\chi_g(\vec{\theta})$, the axial chromatic term $\chi_c(\vec{\theta}, E)$ and the field term χ_f . This term is generally neglected by assuming isoplanatic conditions. In this case, the total phase shift $\chi_t = \chi_g + \chi_c$ depends only on the aperture angle $\vec{\theta}$ of the objective lens and the relative starting energy

$$\kappa = E/E_m, \quad E_m = \langle E \rangle + e\Phi_0. \quad (9)$$

Here Φ_0 is the acceleration voltage. The field term χ_f of the phase shift (8) accounts for the effect of the off-axial geometrical aberrations, such as coma, image curvature, field astigmatism and chromatic field aberrations. The axial term $\chi_g + \chi_c$ of the phase shift (8) considers the aperture aberrations and the axial chromatic aberration. The aperture aberrations produce the standard phase shift $\chi_g = \chi_g(\vec{\theta})$, which is solely a function of the two components θ_x and θ_y of the aperture angle $\vec{\theta}$. The axial chromatic aberration introduces the chromatic contribution $\chi_c = \chi_c(\vec{\theta}, E)$, which is a function of the aperture angle and of the energy deviation E of the incident electron from the mean beam energy E_m .

The electron wave $\psi_f = \psi(z_f, \vec{\theta}, \vec{\theta})$ at the back-focal plane z_f depends on the two-dimensional angular vector of incidence $\vec{\theta}$

and on the aperture angle vector $\vec{\theta}$. Only in the case of single scattering is $\psi_f = \psi(z_f, \vec{\theta} - \vec{\Theta})$ solely a function of the scattering angle $\vec{\theta} - \vec{\Theta}$. Considering the expressions (4)–(7) and assuming the non-isoplanatic case, we obtain the relation

$$\begin{aligned} \psi_f &\approx \frac{1}{i\lambda} \iint P(\vec{r}_f, \vec{\rho}_e) \psi_e(\vec{\rho}_e, \vec{\Theta}) d^2 \vec{\rho}_e \\ &\approx \frac{e^{ik(z_f - z_e)}}{i\lambda f_o} \iint e^{-i\chi(\vec{\theta}, \vec{\rho}_e, E)} e^{-ik\vec{\theta} \cdot \vec{\rho}_e} \psi_e(\vec{\rho}_e, \vec{\Theta}) d^2 \vec{\rho}_e. \end{aligned} \quad (10)$$

The phase shift (8) vanishes if we place the front focal plane of an ideal lens at the exit plane. Only in this case represents the wave function (10) the Fourier transform of the wave at the exit plane up to a constant factor. We introduce the elastic scattering amplitude by assuming a static object potential. In this case, the wave at the exit plane z_e is given by

$$\psi(\vec{r}_e) = T(\vec{r}_e) \psi_0(\vec{r}_e) = \{1 + \Gamma(\vec{r}_e)\} \psi_0(\vec{r}_e). \quad (11)$$

The complex function $T(\vec{r}_e) = 1 + \Gamma(\vec{r}_e)$ represents the object transmission function. This function is complex in the presence of an object and unity when it is absent. Accordingly, the function $\Gamma(\vec{r}_e)$ describes the change of the incident wave after traversing the object. The incident plane wave has the form

$$\psi_0(\vec{r}) = e^{i\vec{K} \cdot \vec{r}}. \quad (12)$$

The direction of incidence is given by the wave vector \vec{K} , which we write in small-angle approximation as

$$\vec{K} \approx k \vec{e}_z + k \vec{\Theta}. \quad (13)$$

Replacing the wave function in the integrand of Eq. (9) by the relations (11) and (12), we obtain

$$\psi_f = \psi_{of} + \frac{e^{ik(z_f - z_e)}}{f_o} e^{-i\chi_e(\vec{\theta}) + \chi_c(\vec{\theta}, \kappa)} f(\vec{\theta}, \vec{\Theta}). \quad (14)$$

The first term on the right hand side represents the non-scattered wave at the back-focal plane

$$\psi_{of} \approx \frac{e^{ikz_f}}{i\lambda f_o} \iint e^{-ik\chi(\vec{\theta}, \vec{\rho}_e, \kappa)} e^{ik(\vec{\Theta} - \vec{\theta}) \cdot \vec{\rho}_e} d^2 \vec{\rho}_e. \quad (15)$$

In the case of the STEM, this wave describes the scanning spot at the object plane. Hence, the size of the diffraction spots at the back-focal plane of the TEM coincides with that of the scanning spot of the STEM.

In the absence of field aberrations we obtain a sharp spot at the position $\vec{\rho}_f = f_o \vec{\theta} = f_o \vec{\Theta}$ in the back-focal plane z_f

$$\psi_{of} \approx \frac{\lambda}{if_o} \delta^2(\vec{\Theta} - \vec{\theta}) e^{ikz_f} e^{-i\chi_c(\vec{\theta}, \kappa)}. \quad (16)$$

Here $\delta^2(\vec{\Theta} - \vec{\theta})$ denotes the two-dimensional delta function. We can also evaluate the integral (15) analytically for non-isoplanatic conditions if we consider only terms of the phase shift $\chi_f(\vec{\theta}, \vec{\rho}_e)$, which are linear and/or bilinear in the components x_e, y_e of the lateral position vector $\vec{\rho}_e$ at the exit plane. These terms comprise the third-order coma, image curvature and field astigmatism as well as the off-axial second-order misalignment aberrations.

The second term on the right hand side of the relation (14) describes the scattered waves at the back-focal plane. Owing to the aberrations of the objective lens, the integral expression

$$f(\vec{\theta}, \vec{\Theta}) = \frac{1}{i\lambda} \iint \Gamma(\vec{\rho}_e, \vec{\Theta}) e^{-i\chi_f(\vec{\rho}_e, \vec{\theta})} e^{-ik(\vec{\theta} - \vec{\Theta}) \cdot \vec{\rho}_e} d^2 \vec{\rho}_e. \quad (17)$$

of the modified scattering amplitude $f(\vec{\theta}, \vec{\Theta})$ differs from the standard scattering amplitude $f(\vec{\theta}, \vec{\Theta})$ for the field-free space by the

phase factor $\exp\{-i\chi_f(\vec{\rho}_e, \vec{\theta})\}$ in the integrand. This factor results from the geometrical lens defects which introduce aberrations at the diffraction plane and at the image plane. However, a distinct lens defect produces generally different aberrations at these planes. For example, the phase shift of the third-order coma introduces a coma at the image plane, yet a distortion at the diffraction plane. The aperture aberrations behave differently because they do not affect the diffraction pattern. The same holds true for the terms of the phase shift which depend solely on the coordinates of the exit plane. This phase shift introduces an aperture aberration at the diffraction plane broadening the Bragg spots of largely extended crystalline specimens. The introduction of the modified scattering amplitude (17) allows one to establish relatively easily a non-isoplanatic theory of image formation.

4. Wave at the Gaussian image plane

To obtain the wave at the image plane z_i , we employ again the generalized Sommerfeld diffraction formula [17], giving

$$\psi_i = \psi(\vec{r}_i) \approx \frac{1}{i\lambda} \iint A(\vec{\rho}_f) e^{-i\chi_p(\vec{\rho}_f)} P_{fi}(\vec{\rho}_i, \vec{\rho}_f) \psi(\vec{\rho}_f) d^2 \vec{\rho}_f. \quad (18)$$

We include the effect of an obstruction-free Zernike phase plate at the back-focal plane of the objective lens by the phase factor $\exp[-i\chi_p(\vec{\rho}_f)]$ although the actual phase plate will be placed at an anamorphic image of this plane. The aperture function $A(\vec{\rho}_f)$ considers the removal of electrons by a diaphragm. Accordingly, the aperture function is unity within the hole of the diaphragm and zero elsewhere.

The elementary wave propagating from the point $\vec{\rho}_f$ in the back-focal plane z_f to the image plane z_i is given by the propagator

$$P_{fi} \approx \frac{e^{iS(\vec{\rho}_i, \vec{\rho}_f)/h}}{Mf_o}. \quad (19)$$

where $S(\vec{\rho}_i, \vec{\rho}_f)/hk$ is the optical path length of the electron travelling along the classical trajectory from the point \vec{r}_f to the point \vec{r}_i ; M denotes the magnification of the image. Neglecting the effect of the projector lenses, we obtain in the case of high magnification $M = (z_i - z_f)/f_o \gg 1$ the relation

$$S(\vec{\rho}_i, \vec{\rho}_f) \approx k \left[z_i - z_f - \frac{\vec{\rho}_i \cdot \vec{\rho}_f}{z_i - z_f} \right] = k(z_i - z_f - \vec{\theta} \cdot \vec{\rho}_i / M). \quad (20)$$

Using this approximation and considering that $\vec{\theta} = \vec{\rho}_f / f_o$, we can rewrite the expression (18) for the wave function at the image plane in the usual form as

$$\psi_i \approx \frac{f_o}{i\lambda M} e^{ik(z_i - z_f)} \iint A(\vec{\theta}) e^{-i\chi_p(\vec{\theta})} e^{-ik\vec{\theta} \cdot \vec{\rho}_i / M} \psi_f(\vec{\theta}, \vec{\Theta}, E) d^2 \vec{\theta}. \quad (21)$$

For reasons of mathematical simplicity, we combine the phase shift $\chi_p(\vec{\theta})$ of the phase plate with the phase shift introduced by the aperture aberrations of the objective lens resulting in the total phase shift

$$\begin{aligned} \chi_t(\vec{\theta}, E) &= \chi_a(\vec{\theta}) + \chi_c(\vec{\theta}, E), \\ \chi_a(\vec{\theta}) &= \chi_g(\vec{\theta}) + \chi_p(\vec{\theta}). \end{aligned} \quad (22)$$

Substituting the expression (14) for ψ_f in (21) and considering the relation (16), we obtain the elastic wave function at the image plane for isoplanatic conditions in the form

$$\begin{aligned} \psi_i &\approx -\frac{e^{ikz_i}}{M} A(\vec{\Theta}) e^{-i\chi_t(\vec{\Theta}, E)} e^{-ik\vec{\Theta} \cdot \vec{\rho}_i / M} \\ &\quad + \frac{e^{ikz_i}}{i\lambda M} \iint A(\vec{\theta}) f(\vec{\theta}, \vec{\Theta}) e^{-ik\vec{\theta} \cdot \vec{\rho}_i / M} e^{-i\chi_t(\vec{\theta}, E)} d^2 \vec{\theta}. \end{aligned} \quad (23)$$

The expression becomes more involved in the general case of non-isoplanatic imaging caused by the field aberrations. Fortunately, we can neglect the effect of these aberrations because (a) the field of view is relatively small in the case of high magnification and (b) the aplanatic TEM aberration correctors also compensate for the off-axial coma.

In order to have an expression, which does not depend on the magnification, it is advantageous to refer the current density distribution in the image plane ψ_i/ψ_i^* back to the object plane. We achieve this by introducing the reduced lateral position vector $\vec{\rho} = \vec{\rho}_i/M$.

Neglecting the inelastic scattering and considering that $A(\vec{\theta})^2 = A(\vec{\theta})$, we derive from (23) for the normalized elastic image intensity the expression

$$\begin{aligned}
 i_{el}(\vec{\rho}, \vec{\theta}, E) &= \psi_i \psi_i^* M^2 \\
 &= A(\vec{\theta}) - \frac{2}{\lambda} \text{Im} \left[A(\vec{\theta}) e^{i\chi_c(\vec{\theta}, E)} \iint A(\vec{\theta}) f(\vec{\theta}, \vec{\theta}) e^{-i\chi_c(\vec{\theta}, E)} e^{ik(\vec{\theta} - \vec{\theta}) \cdot \vec{\rho}} d^2 \vec{\theta} \right] \\
 &\quad + \frac{1}{\lambda^2} \left| \iint A(\vec{\theta}) f(\vec{\theta}, \vec{\theta}) e^{-i\chi_c(\vec{\theta}, E)} e^{-ik \vec{\theta} \cdot \vec{\rho}} d^2 \vec{\theta} \right|^2. \tag{24}
 \end{aligned}$$

The first term on the right hand side accounts for the normalized image intensity without an object. The second term describes the phase contrast for monochromatic plane-wave illumination produced by interference of the scattered wave with the non-scattered wave. Both terms vanish for tilted-illumination or hollow-cone dark-field imaging because $A(\vec{\theta}) = 0$ for $\theta > \theta_0$. The third term causes the so-called scattering contrast. The corresponding intensity is non-linear with respect to the scattering amplitude and results from the elastically scattered electrons which pass through the hole of the beam-limiting aperture. Note that only part of the *scattering absorption contrast* arises from the removal of the scattered electrons by the diaphragm. Therefore, we define the contrast arising from non-linear term of (24) as *scattering contrast*.

To further simplify the calculations, we assume in addition to isoplanatism that the chromatic aberration is rotationally symmetric. In this case, the chromatic phase shift has the standard form

$$\chi_c(\vec{\theta}, E) = \frac{k}{2} \frac{E}{E_0} C_c \theta^2. \tag{25}$$

5. Inelastic scattering and optical theorem

We incorporate the contribution of the inelastic scattered electrons to the image intensity by considering that an inelastic scattered wave can only interfere with another wave if they are both attributed to the same excited state of the object. Hence, electron waves belonging to different final states of the object are incoherent. The incident electron loses the energy E_n by exciting the object from its ground state $|0\rangle$ to the excited state $|n\rangle$. We assume that this energy loss is small compared with the mean energy E_0 of the incident electron beam. In this case, the additional chromatic phase shift of the partial wave ψ_n belonging to the state $|n\rangle$ is

$$\chi_{cn} = \frac{k E_n}{2 E_0} C_c \theta^2. \tag{26}$$

The corresponding inelastic scattered wave resulting at the back-focal plane of the objective lens is defined by the complex

scattering amplitude f_n , which satisfies the reciprocity relation

$$f_n = f_n(\vec{\theta}, \vec{\theta}, E_n) = f_n(-\vec{\theta}, -\vec{\theta}, -E_n). \tag{27}$$

We obtain this relation by reversing the scattering process with respect to time. In this case, the object is initially in the excited state and after collision in the ground state. Moreover, we have also reversed the direction of flight. The contribution of inelastic scattering $i_{in}(\vec{\rho})$ to the total image intensity

$$i(\vec{\rho}, \vec{\theta}, E) = i_{el}(\vec{\rho}, \vec{\theta}, E) + i_{in}(\vec{\rho}, \vec{\theta}, E) \tag{28}$$

is given by

$$\begin{aligned}
 i_{in}(\vec{\rho}, \vec{\theta}) &= \frac{1}{\lambda^2} \sum_{n=1}^{\infty} \left| \iint A(\vec{\theta}) f_n(\vec{\theta}, \vec{\theta}, E_n) e^{-i\chi_{cn}(\vec{\theta})} \right. \\
 &\quad \left. \times e^{-i\chi_c(\vec{\theta}, E + E_n)} e^{-ik \vec{\theta} \cdot \vec{\rho}} d^2 \vec{\theta} \right|^2. \tag{29}
 \end{aligned}$$

We include the quadratic term of the elastic scattering amplitude in this expression by starting the summation with the ground state ($n=0$). For this purpose we write the elastic scattering amplitude $f(\vec{\theta}, \vec{\theta}) = f_e(\vec{\theta}, \vec{\theta})$ as $f_0(\vec{\theta}, \vec{\theta})$ and consider that $\chi_{c0}=0$. By employing this procedure, the normalized image intensity adopts the form

$$\begin{aligned}
 i(\vec{\rho}, \vec{\theta}, E, E_n) - A(\vec{\theta}) &= -\frac{2}{\lambda} \text{Im} \left[A(\vec{\theta}) e^{i\chi_c(\vec{\theta}, E)} \times \iint A(\vec{\theta}) f_0(\vec{\theta}, \vec{\theta}) e^{-i\chi_c(\vec{\theta}, E)} e^{ik(\vec{\theta} - \vec{\theta}) \cdot \vec{\rho}} d^2 \vec{\theta} \right] \\
 &\quad + \frac{1}{\lambda^2} \sum_{n=0}^{\infty} \left| \iint A(\vec{\theta}) f_n(\vec{\theta}, \vec{\theta}, E_n) e^{-i\chi_{cn}(\vec{\theta})} e^{-i\chi_c(\vec{\theta}, E_n)} e^{-ik \vec{\theta} \cdot \vec{\rho}} d^2 \vec{\theta} \right|^2. \tag{30}
 \end{aligned}$$

The energy loss E_n is zero for the elastic partial wave ($n=0$).

We utilize the expression (30) for obtaining the “optical theorem”. To derive this relation, we neglect within the frame of validity of our approximation back-scattering and assume that each incident electron intersects both the object and the image plane. The corresponding requirement $A(\vec{\theta}) = A(\vec{\theta}) = 1$ implies that we do not place beam-limiting apertures in the region between object and image. Thus, the total current at the image plane must coincide with the total incident current at the object plane. We write this condition in the form

$$\iint [i(\vec{\rho}, \vec{\theta}, E) - 1] d^2 \vec{\rho} = 0. \tag{31}$$

Therefore, the integral of the right-hand side of expression (30) taken over the entire image plane must vanish. We can readily perform this integration by utilizing the representation for the two-dimensional delta function

$$\delta^2(\vec{\omega}) = \frac{1}{\lambda^2} \iint e^{-ik\vec{\omega} \cdot \vec{\rho}} d^2 \vec{\rho}. \tag{32}$$

As a result, we obtain the optical theorem

$$\begin{aligned}
 2\lambda \text{Im} f_0(\vec{\theta}, \vec{\theta}) &= \sum_{n=0}^{\infty} \iint |f_n(\vec{\theta}, \vec{\theta}, E_n)|^2 d^2 \vec{\theta} \\
 &= \sigma_{el} + \sigma_{inel} = \sigma_t. \tag{33}
 \end{aligned}$$

This relation states that the elastic scattering amplitude taken in the forward direction and multiplied by twice the wavelength equals the total scattering cross-section. This cross-section is composed of the elastic scattering cross-section

$$\sigma_{el} = \iint |f_0(\vec{\theta}, \vec{\theta})|^2 d^2 \vec{\theta}, \tag{34}$$

and of the inelastic scattering cross-section

$$\sigma_{inel} = \sum_{n=1}^{\infty} \iint |f_n(\vec{\theta}, \vec{\Theta}, E_n)|^2 d^2 \vec{\theta}. \tag{35}$$

The cross-sections depend on the angle of incidence $\vec{\theta}$, except for spherically symmetric objects such as single atoms. The elastic scattering amplitude acts like a bookkeeper who subtracts the intensity carried away by the scattered waves from the intensity of the incident wave. Hence, the optical theorem is the direct result of the conservation of intensity.

6. Effects of chromatic aberration and size of the effective source

In order to incorporate the effects of chromatic aberration and the finite size of the effective source, we introduce the *mean image intensity*. For reasons of mathematical simplicity, we assume Koehler illumination, which implies that the effective source is imaged into the back-focal plane of the objective lens. As a result, each angle of incidence $\vec{\theta}$ correlates to a distinct point of the incoherent effective source. Hence, plane illuminating waves with different directions of incidence must be added incoherently. We describe the angular illumination in TEM by the function $D(\vec{\Theta})$, which corresponds to the detector function in STEM [18]. For the TEM the illumination function is approximately Gaussian. For reasons of mathematical simplicity we normalize the illumination function such that

$$\iint D(\vec{\Theta}) d^2 \vec{\Theta} = 1. \tag{36}$$

Considering this relation and the expression (1) for the distribution of the emission energy, we find for the averaged current density at the image plane the expression

$$I(\vec{\rho}) = \iiint i(\vec{\rho}, \vec{\Theta}, E) D(\vec{\Theta}) g(E) dE d^2 \vec{\Theta}. \tag{37}$$

By substituting in the integrand the expression (24) for the current density I , we readily find that the elastic image intensity consists of three terms, the uniform background, a linear term with respect to the elastic scattering amplitude and a quadratic term.

We consider the effect of the chromatic aberration on the image intensity by assuming the generalized Maxwell distribution (1) for the energy spread of the incident beam. Within the frame of quantum mechanics, we must average the image intensity over the energy spread of the incident electron beam, as described by Eq. (37). By inserting the relations (24), (25) and (1) into the expression (37), we can perform the integration over the energy spread analytically. For the first term, which is linear in the scattering amplitude, we obtain the complex chromatic envelope function

$$\begin{aligned} E_c &= E_c(\theta^2 - \Theta^2, \langle E \rangle) \\ &= \int g(E) e^{i\chi_c(\Theta, E) - \chi_c(\theta, E)} \\ &\times dE = \frac{1}{b^{n+1} \Gamma(n+1)} \int_0^{\infty} E^n e^{-E/b} e^{\frac{k}{2E_0} C_c (\Theta^2 - \theta^2)} \\ &\times dE = \frac{1}{[1 + i(\theta^2 - \Theta^2)/\theta_c^2]^{n+1}}. \end{aligned} \tag{38}$$

The chromatic damping angle θ_c is given by the expression

$$\frac{1}{\theta_c^2} = \frac{k}{2\sqrt{n+1}} \kappa C_c, \quad \kappa = \frac{b}{E_0} \sqrt{n+1} = \frac{\Delta E}{E_0} = \frac{\langle E \rangle}{\sqrt{n+1} E_0}. \tag{39}$$

We rewrite the complex damping function (38) as the product of an amplitude term and a complex phase term, giving

$$E_c = \frac{1}{[1 + i(\theta^2 - \Theta^2)/\theta_c^2]^{n+1}} = |E_c| e^{i\langle \chi_c \rangle} = \frac{e^{i\langle \chi_c \rangle}}{[1 + (\theta^2 - \Theta^2)^2/\theta_c^4]^{(n+1)/2}}. \tag{40}$$

The phase shift

$$\begin{aligned} \langle \chi_c \rangle &= (n+1) \arctan\left(\frac{\theta^2 - \Theta^2}{\theta_c^2}\right) \\ &= (n+1) \arctan\left(\frac{k C_c}{2(n+1) E_0} (\theta^2 - \Theta^2)\right) \\ &\approx \frac{k \langle E \rangle}{2 E_0} C_c (\theta^2 - \Theta^2) - \frac{k^3 C_c^3}{24(n+1)^2} \left(\frac{\langle E \rangle}{E_0}\right)^3 (\theta^2 - \Theta^2)^3 + \dots \end{aligned} \tag{41}$$

accounts for the defocus and the spherical aberrations of electrons with an average energy deviation $\langle E \rangle$. The formula (40) demonstrates that in the case of a Maxwell distribution ($n=1/2$) the absolute value of the chromatic damping envelope

$$|E_c| = [1 + (\theta^2 - \Theta^2)^2/\theta_c^4]^{-(n+1)/2} \tag{42}$$

decreases only proportional to θ^{-3} for large aperture angles $\theta > \theta_c \gg \Theta$. This result differs significantly from that of the standard Gaussian energy distribution. The chromatic envelope of this standard distribution exhibits an unrealistic strong exponential damping with an exponent proportional to $(\theta^2 - \Theta^2)^2$.

The first relation on the right hand side of (41) shows that the mean chromatic defocus is given by

$$\Delta f_c = \frac{\langle E \rangle}{E_0} C_c. \tag{43}$$

Moreover, the power series reveals that the chromatic phase shift also contributes to the phase shift resulting from the geometric aberrations. The chromatic phase shift is zero along the so-called achromatic circle $\theta^2 - \Theta^2 = 0$. This condition is fulfilled if the two-dimensional scattering angle $\vec{\omega} = \vec{\theta} - \vec{\Theta}$ satisfies the relation

$$\vec{\omega}(\vec{\omega} + 2\vec{\Theta}) = 0. \tag{45}$$

The circle shrinks to a point on the optic axis in the case of parallel illumination $\vec{\Theta} = 0$.

In order to obtain the average over the energy distribution of the non-linear terms, we must evaluate the integral

$$E_{cm} = E_c(\theta^2 - \theta'^2, \langle E \rangle) = \int g(E) e^{i\chi_c(\theta', E) - \chi_c(\theta, E)} dE. \tag{46}$$

We readily obtain the result of the integration from that for the linear term by substituting in the expressions (39), (41) and (42) the aperture angle θ' for the angle of incidence θ , giving the *mutual chromatic envelope*

$$\begin{aligned} E_{cm} &= \frac{1}{[1 + i(\theta^2 - \theta'^2)/\theta_c^2]^{n+1}} = |E_{cm}| e^{i\langle \chi_{cm} \rangle} \\ &= \frac{e^{i\langle \chi_{cm} \rangle}}{[1 + (\theta^2 - \theta'^2)^2/\theta_c^4]^{(n+1)/2}}, \end{aligned} \tag{47}$$

$$\langle \chi_{cm} \rangle = (n+1) \arctan\left(\frac{k C_c}{2(n+1) E_0} (\theta^2 - \theta'^2)\right). \tag{48}$$

In the standard case of Koehler illumination, we can describe the incoherent properties of effective source by the standard

Gaussian distribution function

$$D(\vec{\theta}) = D(\theta) = \frac{2}{\theta_s^2} e^{-\theta^2/\theta_s^2}. \tag{49}$$

The characteristic angle $\theta_s \ll \theta_0$ is proportional to the size of the effective source. It follows from the expression (30) that averaging over the angular distribution (49) appreciably affects only the linear term, which produces the phase contrast.

7. TEM bright-field imaging

In the case of bright-field imaging in TEM, the non-scattered beam passes through the openings of all beam limiting apertures. We consider the effect of an obstruction-free phase plate by the phase shift $\chi_p(\theta)$ referred back to the back-focal plane of the objective lens. The phase plate shifts the phase of the scattered wave by a constant value within the region $\theta_p \leq \theta \leq \theta_0$

$$\chi_p(\theta) = \begin{cases} 0 & \text{for } 0 \leq \theta \leq \theta_p \\ \Delta_p & \text{for } \theta_0 \geq \theta > \theta_p \end{cases} \tag{50}$$

The constant phase shift Δ_p can be positive or negative. In the case of axial illumination ($\theta=0$), the phase of the non-scattered wave and that of the small-angle diffracted waves ($\theta < \theta_p$) are not affected by the phase plate.

The properties of an electron micrograph are primarily determined by resolution and contrast. We use the standard definition of light optics for the contrast $C(\vec{\rho})$ of bright-field images:

$$C(\vec{\rho}) = 1 - I(\vec{\rho})/I_0 = 1 - I(\vec{\rho}). \tag{51}$$

The second relation holds because we have normalized the average background intensity to unity ($I_0=1$). The contrast is negative if the image of a point-like object appears as a bright spot, while the contrast is positive if the point object appears in the image as a dark spot on the bright background. By assuming the energy distribution (1) for the incident electrons, we can perform analytically the integration over the energy E in (37), as outlined in the preceding chapter. For tilted plane-wave illumination the image intensity $i(\vec{\rho}, \vec{\theta})$ referred back to the object plane is found as

$$M^2 i(\vec{\rho}, \vec{\theta}) = i_0(\vec{\rho}, \vec{\theta}) = A(\vec{\theta}) + i_1(\vec{\rho}, \vec{\theta}) + i_2(\vec{\rho}, \vec{\theta}), \tag{52}$$

$$i_1(\vec{\rho}, \vec{\theta}) = -\frac{2}{\lambda} \text{Im} \left[e^{i\chi_a(\vec{\theta})} A(\vec{\theta}) \iint A(\vec{\theta}') E_c(\theta^2 - \theta'^2) \times e^{-i\chi_a(\vec{\theta} - \vec{\theta}') \cdot \vec{\rho}} e^{ik(\vec{\theta} - \vec{\theta}') \cdot \vec{\rho}} d^2 \vec{\theta}' \right], \tag{53}$$

$$i_2(\vec{\rho}, \vec{\theta}) = \frac{1}{\lambda^2} \sum_{n=0}^{\infty} \iiint A(\vec{\theta}) A(\vec{\theta}') E_c(\theta^2 - \theta'^2) \times e^{i[\chi_a(\vec{\theta}') - \chi_a(\vec{\theta})]} \times e^{i[\chi_{cn}(\theta^2) - \chi_{cn}(\theta'^2)]} f_n(\vec{\theta}, \vec{\theta}', E_n) f_n^*(\vec{\theta}', \vec{\theta}, E_n) \times e^{ik(\vec{\theta}' - \vec{\theta}) \cdot \vec{\rho}} d^2 \vec{\theta}' d^2 \vec{\theta}. \tag{54}$$

The image intensity (52) consists of three terms. The first term $A(\vec{\theta}) = i_0$ describes the background intensity in the absence of an object. This intensity is unity for bright-field imaging and zero for the dark-field mode. The second term (53) is linear in the elastic scattering amplitude. This term accounts for the phase contrast and for the so-called amplitude contrast which reduces locally the background intensity. In the case of ideal imaging ($\chi_a = \langle \chi_c \rangle = 0$), the amplitude contrast arises solely from the imaginary part of the elastic scattering, whereas the phase contrast vanishes. The third

term (54) describes the part of the scattering contrast formed by the scattered electrons which pass through the hole of the diaphragm. This term contributes the more to the image intensity the larger the hole of the beam-limiting aperture is. The reason for this peculiar behavior stems from the fact that the linear term (53) accounts for the phase contrast and for the amplitude contrast arising from the local reduction of the background intensity by the intensity carried away by the scattered waves. We can separate the intensity distribution (53) in a pure phase contrast intensity $i_p(\vec{\rho}, \vec{\theta})$ and an amplitude contrast intensity. The generalized optical theorem describes an important property of the elastic scattering amplitude, which allows us to express the intensity of the amplitude contrast as a scattering intensity by relating the “anti-Friedel term” of the elastic scattering amplitude with the autocorrelation functions of all scattering amplitudes f_n . For this purpose, we separate the elastic scattering amplitude $f_0 = f_e$ in a selfadjoint “Friedel” term $f_s(\vec{\theta}, \vec{\theta}')$ and an “anti-Friedel” term $f_a(\vec{\theta}, \vec{\theta}')$ as

$$f_e(\vec{\theta}, \vec{\theta}') = f_s(\vec{\theta}, \vec{\theta}') + i f_a(\vec{\theta}, \vec{\theta}'), \tag{55}$$

$$f_s(\vec{\theta}, \vec{\theta}') = [f_e(\vec{\theta}, \vec{\theta}') + f_e^*(\vec{\theta}', \vec{\theta})] / 2, f_a(\vec{\theta}, \vec{\theta}') = [f_e(\vec{\theta}, \vec{\theta}') - f_e^*(\vec{\theta}', \vec{\theta})] / 2i. \tag{56}$$

By considering the reciprocity relation (27), we find that the Friedel and the anti-Friedel term satisfy the relations

$$f_s(\vec{\theta}, \vec{\theta}') = f_s^*(\vec{\theta}', \vec{\theta}) = f_s^*(-\vec{\theta}, -\vec{\theta}'), \tag{57}$$

$$f_a(\vec{\theta}, \vec{\theta}') = f_a^*(\vec{\theta}', \vec{\theta}) = f_a^*(-\vec{\theta}, -\vec{\theta}'). \tag{58}$$

Only if the scattering amplitude is symmetric, $f_e(\vec{\theta}, \vec{\theta}') = f_e(\vec{\theta}', \vec{\theta})$, the Friedel term coincides with the real part and the anti-Friedel term with the imaginary part of the elastic scattering amplitude, respectively. This is the case for single atoms.

The generalized optical theorem connects bilinear the anti-Friedel part (58) of the elastic scattering amplitude with all scattering amplitudes f_n via the relation [18]

$$f_a(\vec{\theta}, \vec{\theta}') \approx \frac{1}{2\lambda} \sum_{n=0}^{\infty} \iint f_n^*(\vec{\theta}', \vec{\theta}, E_n) f_n(\vec{\theta}, \vec{\theta}', E_n) d^2 \vec{\theta}'. \tag{59}$$

We must put $E_0 = E_e = 0$ in the first term ($n=0$) on the right-hand side because the elastically scattered electrons do not suffer an energy loss $E_0 = E_e$. The generalized optical theorem (59) reduces to the standard optical theorem (33) in the special case $\vec{\theta}' = \vec{\theta}$. This theorem demonstrates the non-linear property of the anti-Friedel part of the elastic scattering amplitude because it accounts for the loss of intensity transferred from the incident beam to the scattered beam.

8. Phase contrast for axial illumination

We readily obtain the intensity distribution $j_p(\vec{\rho}, \vec{\theta})$ of the bright-field phase contrast by considering only the Friedel term $f_s(\vec{\theta}, \vec{\theta}')$ of the elastic scattering amplitude in the expression (53) and by setting $A(\vec{\theta}) = 1$. In the following, we consider the special case of axial illumination ($\vec{\theta} = 0$). Employing these assumptions,

we obtain from (51) and (53) for the phase contrast the expression

$$C_p(\vec{\rho}) = \frac{2}{\lambda} \text{Im} \left[\iint A(\vec{\theta}) E_c(\theta^2) e^{-i\chi_a(\vec{\theta})} f_s(\vec{\theta}, \vec{\Theta} = 0) e^{-ik\vec{\theta}\vec{\rho}} d^2\vec{\theta} \right]. \quad (60)$$

To demonstrate the pure phase nature of the phase contrast, we integrate the expression (60) over the entire image plane. We can readily perform this integration analytically by utilizing the representation of the two-dimensional delta function

$$\delta^2(\vec{\theta}) = \frac{1}{\lambda^2} \iint e^{-ik\vec{\theta}\vec{\rho}} d^2\vec{\rho}. \quad (61)$$

Considering further relation (57) and $\chi_a(0) = 0$, we readily demonstrate that the mean phase-contrast vanishes

$$\iint C_p(\vec{\rho}) d^2\vec{\rho} = 2\lambda \text{Im}[A(0)E_c(0)f_s(0,0)] = 2\lambda \text{Im} f_s(0,0) = 0. \quad (62)$$

The result demonstrates that the phase contrast is formed entirely by constructive and destructive interference between the non-scattered wave and the elastically scattered partial waves emanating from the constituent atoms of the object. Accordingly, the sum of the resulting intensity fluctuations must vanish. We obtain this result by considering only the Friedel term of the elastic scattering amplitude.

It is advantageous to describe the transfer properties of the electron optical system by means of the Fourier transform of the contrast. Considering the definitions (22), we obtain for the Fourier transform of the phase contrast (60) the relation

$$\begin{aligned} \tilde{C}_p(\vec{\omega}) &= \iint C_p(\vec{\rho}) e^{ik\vec{\omega}\vec{\rho}} d^2\vec{\rho} \\ &= \frac{1}{i\lambda} |E_c(\omega^2)| A(\omega) \\ &\quad \times \left[e^{-i\langle\chi_c(\omega^2)\rangle} e^{-i[\chi_p(\omega) + \chi_g(\vec{\omega})]} f_s(\vec{\omega}, 0) - e^{i\langle\chi_c(\omega^2)\rangle} \right. \\ &\quad \left. \times e^{i[\chi_p(\omega) + \chi_g(-\vec{\omega})]} f_s^*(-\vec{\omega}, 0) \right]. \end{aligned} \quad (63)$$

By employing (57) together with $\vec{\Theta} = 0$, we can rewrite the right hand side of expression (63) as the product of a phase contrast transfer function $K_p(\vec{\omega}) = K_p(\vec{\omega}, \vec{\Theta} = 0)$ and the Friedel part of the elastic scattering amplitude

$$\tilde{C}_p(\vec{\omega}) = 2\lambda K_p(\vec{\omega}) f_s(\vec{\omega}, 0). \quad (64)$$

The phase contrast transfer function is complex and is given by

$$\begin{aligned} K_p(\vec{\omega}) &= -i |E_c(\omega^2)| A(\omega) [e^{-i\langle\chi_c(\omega^2)\rangle} e^{-i[\chi_p(\omega) + \chi_g(\vec{\omega})]} \\ &\quad - e^{i\langle\chi_c(\omega^2)\rangle} e^{i[\chi_p(\omega) + \chi_g(-\vec{\omega})]}]. \end{aligned} \quad (65)$$

This function is only real if the phase shift produced by the geometrical aberrations is symmetric ($\chi_g(-\vec{\omega}) = \chi_g(\vec{\omega})$), which implies that the residual aberrations of even order are negligibly small. In this case, the phase contrast transfer function adopts the form

$$K_p(\vec{\omega}) = - |E_c(\omega^2)| A(\omega) \sin[\chi_p(\omega) + \chi_g(\vec{\omega}) + \langle\chi_c(\omega^2)\rangle]. \quad (66)$$

The transfer function (66) also considers the phase-shift (50) introduced by an obstruction-free phase plate. By taking into account the relations (50) and (23), we find for the phase contrast transfer function the expression

$$\begin{aligned} K_p(\vec{\omega}) &= - |E_c(\omega^2)| \\ &\quad \times \begin{cases} \sin[\chi_g(\vec{\omega}) + \langle\chi_c(\omega^2)\rangle] & \text{for } 0 \leq \omega \leq \theta_p \\ A(\omega) \sin[\Delta_p + \chi_g(\vec{\omega}) + \langle\chi_c(\omega^2)\rangle] & \text{for } \theta_p < \omega \leq \theta_0 \end{cases} \end{aligned} \quad (67)$$

The correction of the axial chromatic and geometrical aberrations by means of an appropriate corrector enables us to nullify the phase shifts $\langle\chi_c(\omega^2)\rangle$, $\chi_g(\vec{\omega})$ and to realize a uniform chromatic damping envelope $|E_c| = 1$. In this case, the phase contrast transfer function reduces to the simple form

$$K_p(\vec{\omega}) = K_p(\omega) = \begin{cases} 0 & \text{for } 0 \leq \omega \leq \theta_p \\ -\sin\Delta_p & \text{for } \theta_p < \omega \leq \theta_0 \end{cases}. \quad (68)$$

We obtain maximum positive phase contrast by choosing $\Delta_p = -\pi/2$ and maximum negative phase contrast by choosing $\Delta_p = \pi/2$. To enable the transfer of a large range of spatial frequencies λ/ω , the ratio θ_0/θ_p should be made as large as possible. The smallest achievable angle θ_p is limited by the geometry of the phase plate. If the corrector compensates only for the geometrical axial aberrations, the maximum usable aperture angle $\theta_0 = \theta_c$ is determined by the chromatic damping envelope (40). Its characteristic angle θ_c determines the information limit $d_i \approx \lambda/\theta_c$. We assume a Maxwell energy distribution ($n=1/2$) and define the information limit by postulating that the chromatic damping envelope has decreased to about 12.5% of its maximum value. Employing these assumptions and the relations (39) and (3), we derive for the information limit of a spherical aberration corrected electron microscope the expression

$$d_i \approx 0.56 \sqrt{\lambda C_c \Delta E / E_0}. \quad (69)$$

This result is somewhat inaccurate because it relies on the definition of the minimum value of the damping amplitude that sets the limit for the highest detectable spatial frequency. For example, the information limit reduces by about a factor 0.74 if we choose 5% instead of 12.5% of the maximum value one of the damping amplitude. We do not obtain such a reduction in the case of a Gaussian energy distribution due to the unrealistic strong decrease of the chromatic damping amplitude.

The phase contrast vanishes for homogeneous incoherent full-cone illumination if the maximum cone angle Θ_0 equals the limiting objective aperture angle θ_0 . In this case, we have the relation

$$D(\vec{\Theta}) A(\vec{\Theta}) = A(\vec{\Theta}) / \Omega_0, \quad \Omega_0 = \pi \Theta_0^2 = \pi \theta_0^2 \quad (70)$$

By employing the expressions (37), (51) and considering only the Friedel term (57) of the elastic scattering amplitude (55), we eventually obtain

$$\begin{aligned} C_p(\vec{\rho}) &= - \iint i_p(\vec{\rho}, \vec{\Theta}) D(\Theta) d^2\vec{\Theta} \\ &= \frac{1}{\lambda \Omega_0} \text{Im} \left[\iint \iint A(\vec{\Theta}) A(\vec{\theta}) E_c(\theta^2 - \Theta^2) \right. \\ &\quad \left. \times e^{i[\chi_a(\vec{\Theta}) - \chi_a(\vec{\theta})]} f_s(\vec{\theta}, \vec{\Theta}) e^{ik\vec{\rho}(\vec{\Theta} - \vec{\theta})} d^2\vec{\theta} d^2\vec{\Theta} \right] = 0. \end{aligned} \quad (71)$$

We derived the last relation by considering that the result of the fourfold integration is real. In order to demonstrate this behavior, we split up the integrand into two identical halves and exchange in one half the integration variables $\vec{\theta}$ and $\vec{\Theta}$. By employing the relations $E_c(\Theta^2 - \theta^2) = E_c^*(\theta^2 - \Theta^2)$ and $f_s(\vec{\Theta}, \vec{\theta}) = f_s^*(\vec{\theta}, \vec{\Theta})$, we find that the resulting expression represents the conjugate complex of the first half of the integrand. Since the sum of the two terms is real, its imaginary part is zero. We eliminate the phase contrast in practice by means of critical illumination. In this case, we image the effective source into the object plane. In order to achieve the required illumination angle, it is necessary to appropriately magnify the image of the effective source. In order to avoid large magnifications, we need a sufficiently extended effective source to illuminate incoherently a large object field.

Nevertheless, we can also eliminate the phase contrast in the case of a coherent source, for example a field emitter. Critical illumination is employed in scanning transmission electron microscopes (STEM) equipped with a highly coherent gun. Accordingly, the illuminated area is very small and given by the spot size of the focused beam. By scanning the beam over the required field of view and employing a bright-field detector with maximum detection angle $\theta_m = \theta_0$, we approximately realize a self-luminous object because the phase contrast vanishes.

9. Amplitude contrast, scattering contrast and scattering absorption contrast

The scattering contrast C_s is formed by the quadratic terms of the scattering amplitudes whereas the interference of the anti-Friedel term of the elastically scattered wave with the non-scattered wave produces the amplitude contrast C_a . This definition is somewhat misleading, because a significant part of the scattering absorption contrast results from the aberrations of the lenses. As a result, electrons emanating from a distinct point of the exit plane miss the conjugate image point. The contrast produced by aberrations and diffraction largely surpasses that resulting from absorption by the diaphragm. The anti-Friedel term of the elastic scattering amplitude always reduces the bright field intensity because it accounts for the loss of intensity of the primary wave. This intensity equals the intensity of all scattered waves.

To elucidate the effect of the anti-Friedel term, we consider the bright-field image of a thin object in an ideal TEM equipped with an imaging energy filter. If we turn off the filter and remove the absorbing diaphragm, the contrast vanishes in the Gaussian image plane because all scattered electrons originating from an object point are redirected by the aberration-free lenses into the conjugate image point. By removing the inelastic scattered electrons with the energy filter, a “shadow” image appears which represents the non-local inelastic interaction potential. The positive contrast of the inelastic shadow image results from the destructive interference of the elastically scattered wave with the primary wave. Therefore, even in the case of real lenses, the image is not affected by the energy losses of the inelastic scattered electrons. The inelastic shadow image in a chromatic-aberration-corrected TEM corresponds to the “inelastic” image formed in the STEM using all inelastic scattered electrons.

The scattering absorption contrast $C_{sa} = C_s + C_a$ is the sum of scattering contrast and amplitude contrast. By employing relations (51)–(56), we eventually obtain the expression

$$C_{sa}(\vec{\rho}, \vec{\theta}) = \frac{2}{\lambda} \text{Re} \left[A(\vec{\theta}) e^{i\chi_a(\vec{\theta})} \iint A(\vec{\theta}') e^{-i\chi_a(\vec{\theta}')} \times E_c(\theta^2 - \theta'^2) f_a(\vec{\theta}, \vec{\theta}') e^{ik(\vec{\theta} - \vec{\theta}') \cdot \vec{\rho}} d^2 \vec{\theta}' \right] - \frac{1}{\lambda^2} \sum_{n=0}^{\infty} \iint \iint A(\vec{\theta}) A(\vec{\theta}') e^{i[\chi_a(\vec{\theta}') - \chi_a(\vec{\theta})]} \times E_c(\theta^2 - \theta'^2) \times e^{i[\chi_n(\theta') - \chi_n(\theta)]} f_n(\vec{\theta}, \vec{\theta}', E_n) \times f_n^*(\vec{\theta}', \vec{\theta}, E_n) e^{ik(\vec{\theta} - \vec{\theta}') \cdot \vec{\rho}} d^2 \vec{\theta}' d^2 \vec{\theta}'. \tag{72}$$

The first term vanishes if $A(\theta) = 0$, which is the case for dark-field imaging. The second term is always negative and formed by the scattered electrons which pass through the hole of the aperture diaphragm.

To survey the transfer of the spatial frequencies $\vec{\omega}/\lambda$ contributing to the scattering absorption contrast, we take the two-dimensional Fourier transform of the expression (70) with

respect to $\vec{\rho}$, giving

$$\tilde{C}_{sa}(\vec{\omega}, \vec{\theta}) = \iint C_{sa}(\vec{\rho}, \vec{\theta}) e^{-ik\vec{\omega} \cdot \vec{\rho}} d^2 \vec{\rho} = +\lambda A(\vec{\theta}) \left[A(\vec{\theta} + \vec{\omega}) e^{i\chi_a(\vec{\theta})} e^{-i\chi_a(\vec{\theta} + \vec{\omega})} \times E_c(\omega^2 + 2\vec{\omega} \cdot \vec{\theta}) f_a(\vec{\theta} + \vec{\omega}, \vec{\theta}) + A(\vec{\theta} - \vec{\omega}) e^{-i\chi_a(\vec{\theta})} e^{i\chi_a(\vec{\theta} - \vec{\omega})} \times E_c^*(\omega^2 - 2\vec{\omega} \cdot \vec{\theta}) f_a^*(\vec{\theta} - \vec{\omega}, \vec{\theta}) \right] - \sum_{n=0}^{\infty} \iint A(\vec{\theta} + \vec{\omega}) A(\vec{\theta}') e^{i[\chi_a(\vec{\theta}') - \chi_a(\vec{\theta} + \vec{\omega})]} \times E_c(\omega^2 + 2\vec{\omega} \cdot \vec{\theta}') e^{i[\chi_n(\theta') - \chi_n(\vec{\theta} + \vec{\omega})]} \times f_n(\vec{\theta} + \vec{\omega}, \vec{\theta}') f_n^*(\vec{\theta}, \vec{\theta}') d^2 \vec{\theta}'. \tag{73}$$

For simplicity we have introduced the notation $f_n(\vec{\theta}, \vec{\theta}') = f_n(\vec{\theta}, \vec{\theta}', E_n)$.

10. Scattering absorption contrast for parallel axial illumination

We first consider the standard case of parallel axial illumination ($\theta = 0$) and a circular aperture opening. By setting $A(\theta = 0) = 1$, $A(-\vec{\omega}) = A(\vec{\omega}) = A(\omega)$ and using the relation (58), we obtain for the Fourier transform of the scattering absorption contrast the relation

$$\tilde{C}_{sa}(\vec{\omega}, 0) = \tilde{C}_a(\vec{\omega}, 0) - \tilde{C}_{s2}(\vec{\omega}, 0), \tag{74}$$

$$\tilde{C}_a(\vec{\omega}, 0) = 2\lambda A(\omega) \text{Re}[e^{-i\chi_a(\vec{\omega})} E_c(\omega^2)] f_a(\vec{\omega}, 0) = 2\lambda K_a(\vec{\omega}) f_a(\vec{\omega}, 0), \tilde{C}_{s2}(\vec{\omega}, 0) = \sum_{n=0}^{\infty} \iint A(\vec{\omega} + \vec{\omega}') A(\omega) e^{i[\chi_a(\vec{\omega}') - \chi_a(\vec{\omega})]} \times E_c(\omega^2 + 2\vec{\omega} \cdot \vec{\omega}') e^{i[\chi_n(\omega') - \chi_n(\omega)]} f_n(\vec{\omega} + \vec{\omega}', 0) f_n^*(\vec{\omega}, 0) d^2 \vec{\omega}'. \tag{75}$$

The term $\tilde{C}_a(\vec{\omega}, 0)$ represents the Fourier transform of the image contrast produced by the interference of the anti-Friedel part of the elastic scattering wave with the incident wave. This term accounts for the reduction of the uniform background intensity by the removing scattered electrons by the diaphragm and the imaging energy filter.

The amplitude contrast transfer function is given by

$$K_a(\vec{\omega}) = A(\omega) |E_c(\omega^2)| \cos[\chi_a(\vec{\omega}) + \langle \chi_c \rangle]. \tag{76}$$

Considering relations (23) and (47), we find

$$K_a(\vec{\omega}) = |E_c(\omega^2)| \times \begin{cases} \cos[\chi_g(\vec{\omega}) + \langle \chi_c \rangle] & \text{for } 0 \leq \omega \leq \theta_p \\ A(\omega) \cos[A_p + \chi_g(\vec{\omega}) + \langle \chi_c \rangle] & \text{for } \omega > \theta_p \end{cases} \tag{77}$$

We can easily compensate for the phase shift $\langle \chi_c \rangle$ by choosing the defocus (43). The amplitude contrast function in forward direction ($\omega = 0$) is unity: $K_a(0) = 1$.

For an ideal microscope operating without a phase plate ($\Delta_p = 0$, $\theta_p = 0$, $\chi_a = 0$, $E_c = 1$), the amplitude contrast transfer function equals the aperture function $A(\omega)$, and the phase contrast

transfer function (66) is zero. In this case, the contrast in the Gaussian image plane is a pure scattering absorption contrast given by

$$C_s(\vec{\rho}) = \frac{1}{\lambda^2} \iint \tilde{C}_s(\vec{\omega}, 0) e^{ik\vec{\omega}\vec{\rho}} d^2\vec{\omega}. \tag{78}$$

By employing the relation (58) for the anti-Friedel part of the elastic scattering amplitude, we obtain the contrast in the Gaussian image plane of an ideal microscope for parallel axial illumination as

$$\begin{aligned} C_{sa}(\vec{\rho}) &= \frac{1}{\lambda^2} \sum_{n=0}^{\infty} \iint A(\omega) e^{-ik\vec{\omega}\vec{\rho}} \iint [f_n(\vec{\theta}, 0) f_n^*(\vec{\theta}, \vec{\omega}) \\ &\quad - A(\vec{\theta} + \vec{\omega}) f_n(\vec{\theta} + \vec{\omega}, 0) f_n^*(\vec{\theta}, 0)] d^2\vec{\theta} d^2\vec{\omega} \\ &= \frac{1}{\lambda^2} \sum_{n=0}^{\infty} \iint A(\omega) e^{-ik\vec{\omega}\vec{\rho}} \iint f_n(\vec{\theta}, 0) f_n^*(\vec{\theta}, \vec{\omega}) \\ &\quad - A(\vec{\theta}) f_n^*(\vec{\theta} - \vec{\omega}, 0) d^2\vec{\theta} d^2\vec{\omega}. \end{aligned} \tag{79}$$

We have derived the last integral expression by substituting $\vec{\theta}$ for $\vec{\theta} + \vec{\omega}$ in the second term of the integrand of the first integral.

High-resolution imaging requires a large-angle aperture. As a result, most of the electrons, which have been removed from the primary beam by elastic or inelastic scattering, are meticulously redirected by the ideal lens. Hence, almost no shadow will be found in the place where the image of a scattering object should be. In the absence of a beam limiting aperture, the contrast (79) vanishes within the frame of validity of the first-order Born approximation, which satisfies Friedel's law

$$f_n(\vec{\theta}, \vec{\omega}) \approx f_n^{(1)}(\vec{\theta} - \vec{\omega}). \tag{80}$$

The second identity holds because Born's first-order approximation of the scattering amplitude depends only on the scattering vector $k_n(\vec{\theta} - \vec{\omega})$. In order to produce an appreciable contrast in the ideal Gaussian image plane, we must incorporate a phase plate at the back-focal plane of the objective lens or at a magnified image of this plane, respectively.

11. Incoherent bright-field imaging

To obtain maximum scattering absorption contrast, we apply critical illumination such that the limiting illumination angle Θ_0 equals the aperture angle θ_0 . In this case, the phase contrast (68) vanishes, as we have shown in the preceding section. Accordingly, the image contrast is a pure scattering absorption contrast. After introducing the expression (58) for $f_a(\vec{\theta}, \vec{\Theta})$ in (69) and considering (67), the contrast becomes

$$\begin{aligned} C(\vec{\rho}) = C_{sa}(\vec{\rho}) &= \iint D(\vec{\Theta}) C_s(\vec{\rho}, \vec{\Theta}) d^2\vec{\Theta} = (1/\Omega_0) \\ &\quad \times \iint A(\Theta) C_{sa}(\vec{\rho}, \vec{\Theta}) d^2\vec{\Theta} \\ &= \frac{1}{\lambda^2 \Omega_0} \text{Re} \sum_{n=0}^{\infty} \iint \iint A(\Theta) A(\theta) e^{i[\chi_a(\vec{\Theta}) - \chi_a(\theta)]} E_c(\theta^2 - \Theta^2) \\ &\quad \times \iint f_n(\vec{\theta}, \vec{\Theta}) f_n^*(\vec{\theta}, \vec{\Theta}) d^2\vec{\theta} \\ &\quad \times e^{ik(\vec{\Theta} - \vec{\theta})\vec{\rho}} d^2\vec{\theta} d^2\vec{\Theta} \\ &\quad - \frac{1}{\lambda^2 \Omega_0} \sum_{n=0}^{\infty} \iint \iint A(\Theta) A(\theta) e^{i[\chi_a(\vec{\Theta}) - \chi_a(\theta)]} E_c(\theta^2 - \Theta^2) \\ &\quad \times e^{i[\chi_c(\vec{\Theta}, E_n) - \chi_c(\vec{\theta}, E_n)]} \times \iint A(\Theta) f_n(\vec{\theta}, \vec{\Theta}) \\ &\quad \times f_n^*(\vec{\theta}, \vec{\Theta}) d^2\vec{\theta} d^2\vec{\Theta} e^{ik(\vec{\Theta} - \vec{\theta})\vec{\rho}} d^2\vec{\theta} d^2\vec{\Theta}. \end{aligned} \tag{81}$$

We can bring this rather lengthy expression in a more compact and lucid form by exchanging in the first sum the vector angles $\vec{\theta}$ and $\vec{\Theta}$. This exchange does not alter the integral because it merely represents a change of notation of the integration variables, giving

$$\begin{aligned} C(\vec{\rho}) &= \frac{1}{\lambda^2 \Omega_0} \text{Re} \sum_{n=0}^{\infty} \iint \iint A(\theta') A(\theta) e^{i[\chi_a(\vec{\Theta}) - \chi_a(\vec{\theta})]} \\ &\quad \times E_c(\theta^2 - \theta'^2) e^{ik(\vec{\Theta} - \vec{\theta})\vec{\rho}} \\ &\quad \times \iint \{ f_n(\vec{\Theta}, \vec{\theta}') f_n^*(\vec{\Theta}, \vec{\theta}) - A(\Theta) f_n(\vec{\theta}, \vec{\Theta}) f_n^*(\vec{\theta}, \vec{\Theta}) \\ &\quad \times e^{i[\chi_c(\vec{\theta}, E_n) - \chi_c(\vec{\Theta}, E_n)]} \} d^2\vec{\theta} d^2\vec{\theta}' d^2\vec{\Theta}. \end{aligned} \tag{82}$$

The first term in the parenthesis accounts for the shadow image produced by the loss of intensity of the primary beam. The missing intensity is taken out by the scattered electrons, which are partly removed from the beam by the aperture diaphragm. The second term accounts for the scattered electrons which pass through the aperture and are redirected by the objective lens. Owing to its chromatic aberration, the inelastic scattered electrons are deflected more strongly than the elastically scattered electrons and blur the shadow image. Within the frame of wave optics, this blurring results from the chromatic phase shift $\chi_{cn}(\vec{\theta}) = \chi_c(\vec{\theta}, E_n)$ suffered by the inelastic partial waves after passing through the field of the objective lens. We can clear up the image by removing the inelastic scattered electrons with an imaging energy filter. In this case, only the elastic term ($n=0$) of the second expression in the parenthesis remains. Note that the filter does not affect the first expression, which results from the anti-Friedel term of the elastic scattering amplitude.

The contrast of the incoherent bright-field image is always positive because it originates primarily from the absorption of the scattered electrons by the aperture-limiting diaphragm. This behavior becomes even more obvious within the frame of validity of the first-order Born approximation, which satisfies Friedel's law (80). Assuming the validity of this approximation, the scattering absorption contrast for incoherent illumination (82) reduces to

$$\begin{aligned} C^{(1)}(\vec{\rho}) &= \frac{1}{\lambda^2 \Omega_0} \sum_{n=0}^{\infty} \iint \iint A(\theta') A(\theta) e^{i[\chi_a(\vec{\theta}') - \chi_a(\vec{\theta})]} E_c(\theta^2 - \theta'^2) e^{ik(\vec{\theta}' - \vec{\theta})\vec{\rho}} \\ &\quad \times \iint f_n^{(1)}(\vec{\theta} - \vec{\Theta}) f_n^{(1)*}(\vec{\theta} - \vec{\Theta}) [1 - A(\Theta) e^{i[\chi_c(\vec{\theta}, E_n) - \chi_c(\vec{\Theta}, E_n)]}] \\ &\quad \times d^2\vec{\Theta} d^2\vec{\theta} d^2\vec{\theta}'. \end{aligned} \tag{83}$$

Relations (82) and (83) demonstrate that the inelastic scattered electrons strongly blur the incoherent image. We can clear the image most effectively by removing these electrons with an imaging energy filter, giving

$$\begin{aligned} C_{sa}^{(1)}(\vec{\rho}) &= \frac{1}{\lambda^2 \Omega_0} \sum_{n=0}^{\infty} \iint \iint A(\theta') A(\theta) e^{i[\chi_a(\vec{\theta}') - \chi_a(\vec{\theta})]} T_c(\theta^2 - \theta'^2) \\ &\quad \times \iint f_n^{(1)}(\vec{\theta} - \vec{\Theta}) f_n^{(1)*}(\vec{\theta} - \vec{\Theta}) [1 - A(\Theta) \delta_{n0}] d^2\vec{\Theta} \\ &\quad \times e^{ik(\vec{\theta}' - \vec{\theta})\vec{\rho}} d^2\vec{\theta}' d^2\vec{\theta}. \end{aligned} \tag{84}$$

The Kronecker symbol δ_{n0} is unity for $n=0$ and zero elsewhere. The contribution of the elastically scattered electrons to the scattering absorption contrast decreases with increasing resolution because the fraction of scattered electrons removed by the aperture becomes smaller the larger the hole is. Therefore, this imaging mode is not appropriate in the case of atomic resolution. For this resolution, the use of negative phase contrast

combined with negative scattering absorption contrast is most advantageous.

12. Optimum bright-field imaging of crystalline objects

We obtain bright-field images of crystalline specimens by employing plane-wave axial illumination ($\Theta=0$). Moreover, we align the crystal such that the electrons are incident along a high-symmetry zone axis. In this case, the incident electrons channel along the atom columns similar to the propagation of light in fiber-optics devices. Because each atom column acts in first approximation like an elongated atom, we can write the elastic scattering amplitude with a sufficient degree of accuracy as

$$f_0(\vec{\theta}, 0) = \sum_v f_{cv}(\theta) e^{ik\vec{\theta} \cdot \vec{\rho}_v} \tag{85}$$

The complex elastic scattering amplitude f_{cv} of each column v depends on the object thickness t , on the number n_{Av} of atoms within each column, on their atomic number Z_v and on the absolute value of the scattering angle $\vec{\theta}$

$$f_{cv}(\vec{\theta}) = f_{cv}(\theta) = |f_{cv}(\theta)| e^{i\eta_v(\theta)} \tag{86}$$

It follows from the optical theorem (33) that the phases of the scattering amplitudes do not vanish in forward direction ($\eta_v(0) \neq 0$). The amplitudes $f_{cv}(\theta)$ can be derived from multi-slice calculations.

To simplify our considerations, we assume zero-loss imaging and a TEM equipped with an obstruction-free phase plate and a corrector compensating for the spherical aberration. In this case, we can consider the phase shift χ_p of the phase plate (50), the defocus Δf and the coefficient of the third-order spherical aberration $C_3=C_3$ as free parameters. The inelastic scattered electrons are removed by an imaging energy filter. The aberration corrector and the phase plate enable us to arbitrarily adjust the phase shift (22) given by

$$\chi_t(\vec{\theta}) = \chi_t(\theta) = \chi_p + \frac{\pi}{2\lambda}(C_3\theta^4 - 2\Delta f\theta^2) + \langle \chi_c \rangle \tag{87}$$

Because the phase shift (87) and the scattering amplitudes (83) depend only on the absolute value of the angular vector $\vec{\theta}$, we can perform in (53) and (54) the integrations over the azimuth angle of this vector analytically. Employing in addition the relations (51) and (52), we eventually obtain for the contrast of the crystalline object the expression

$$C(\vec{\rho}) = C_1(\vec{\rho}) + C_2(\vec{\rho}), \tag{88}$$

$$C_1(\vec{\rho}) = 2k \sum_v \text{Im} \iint A(\theta) |E_c(\theta^2)| |f_{cv}(\theta)| e^{i[\eta_v(\theta) - \chi_t(\theta)]} J_0(k\theta |\vec{\rho} - \vec{\rho}_v|) \theta d\theta, \tag{89}$$

$$C_2(\vec{\rho},) = -k^2 \sum_{\mu, \nu} \iiint A(\vec{\theta}) A(\vec{\theta}') E_c(\theta^2 - \theta'^2) e^{i[\chi_a(\theta') - \chi_a(\theta)]} \times f_{c\nu}(\theta) f_{c\mu}^*(\theta') J_0(k\theta |\vec{\rho} - \vec{\rho}_\nu|) J_0(k\theta' |\vec{\rho} - \vec{\rho}_\mu|) \theta' d\theta' \theta d\theta. \tag{90}$$

The function $J_0(x)$ is the Bessel function of order zero. The scattering contrast (90) is always negative. Hence, to achieve highest contrast for the atom column ν , we must adjust the phase shift (87) in such a way that it satisfies in the angular region $\theta_c \geq \theta \geq \theta_p$ the relation

$$\chi_t(\theta) = \Delta_p + \frac{\pi}{2\lambda}(C_3\theta^4 - 2\Delta f\theta^2) + \langle \chi_c \rangle \approx \eta_\nu(\theta) + \frac{\pi}{2}. \tag{91}$$

Accordingly, the highest achievable contrast is always negative. If the crystalline object is composed of different atoms, it is only possible to maximize the contrast of columns composed of the same kind of atoms. The phase shift $\chi_t(\theta)$ is zero for $\theta=0$.

Because the angle θ_p is very small compared with the limiting aperture angle $\theta_c=\theta_0$, the contrast term (89) consists of a weak positive background term $C_{1b}(\vec{\rho})$ obtained by the integration over the small angular region $0 \leq \theta \leq \theta_p$ and a strong negative high-resolution term $C_{1h}(\vec{\rho})$ resulting from the integration over the region $\theta_c \geq \theta \geq \theta_p$. We can perform the integration analytically for weak background contrast $C_{1b}(\vec{\rho})$ by utilizing the small-angle approximations $\chi_t=0$, $E_c=1$, and considering that $A(\theta)=1$. As a result, we eventually obtain

$$C_{1b}(\vec{\rho}) = \theta_p \sum_v \text{Im} f_{cv}(0) \frac{J_1(k\theta_p |\vec{\rho} - \vec{\rho}_v|)}{|\vec{\rho} - \vec{\rho}_v|} \tag{92}$$

Here $J_1(x)$ is the Bessel function of order 1. Owing to the oscillatory behavior of the Bessel function the contribution (92) to the background contrast fluctuates locally. This variation reduces with decreasing angle θ_p . The mean background contrast is always positive and given by

$$\langle C_{1b} \rangle = \frac{1}{a_o} \iint_{A_r} C_{1b}(\vec{\rho}) d^2\vec{\rho} = \frac{2\lambda}{A_o} \sum_v \text{Im} f_{cv}(0) = \frac{\sigma_t}{A_o} \tag{93}$$

Here a_o is the area of object which is recorded in the image. The total scattering cross-section σ_t is produced by all elastic and inelastic scattering processes within the imaged object area.

This result confirms our conjecture that the uniform bright-field intensity $I_0=1$ will be reduced by the amplitude contrast. Moreover, we can state that the incorporation of an obstruction-free phase shifter and aberration correction enables one to adjust the phase shift Δ_p , the defocus Δf , and the coefficient C_3 of the spherical aberration in such a way that the contrast improves significantly. This possibility is extremely helpful for imaging radiation-sensitive objects.

13. Outline of a suitable obstruction-free phase shifter

Scherzer realized an obstruction-free phase shift of the scattered electron wave by utilizing the phase shift produced by the spherical aberration of the objective lens together with a properly chosen defocus $\Delta f = \Delta f_S = \sqrt{\lambda|C_3|}$ known as *Scherzer focus* [10]. The resulting phase shift χ_s is negative in the useful angular region

$$\theta_p \approx 0.3 \left(\frac{\lambda}{C_3} \right)^{1/4} \leq \theta \leq \theta_0 \approx 1.5 \left(\frac{\lambda}{C_3} \right)^{1/4} \tag{94}$$

Therefore, the Scherzer phase shift χ_s represents roughly an annular Zernike phase plate, which shifts the phase of the scattered wave by about $-\pi/2$ in the region $\theta_p \leq \theta \leq \theta_0$. Unfortunately, the useful relative width $\theta_0/\theta_p = q_{\max}/q_{\min}$ of the phase plate is only about 5. Therefore, only object spatial frequencies $q = \lambda/\theta$ within the range $q_{\min} \leq q \leq q_{\max}$ will contribute appreciably to the phase contrast. In order to increase this domain significantly and to achieve negative phase contrast we need a phase shift $\pi/2$ and a ratio $\theta_0/\theta_p \geq 100$. We can realize these requirements in an aberration-corrected TEM by placing a proper phase shifter in the region behind the first intermediate image of the object whose magnification M must be chosen appropriately.

The useful obstruction-free phase shifter consists of a rectangular phase plate and a telescopic quadrupole system, which forms a single or two orthogonal anamorphic images of the diffraction plane (back-focal plane of the objective lens)

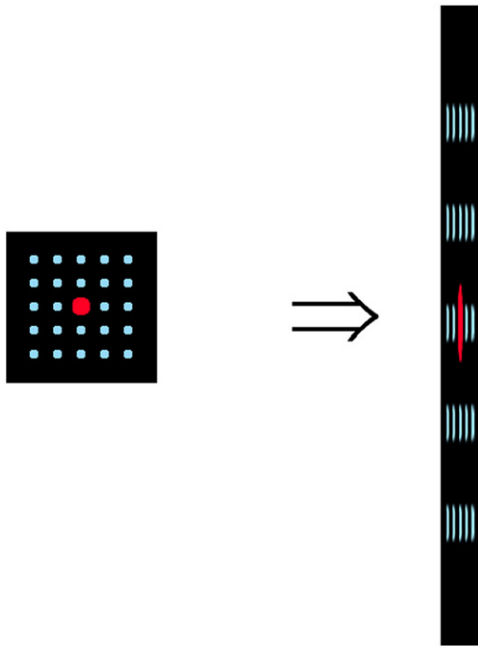


Fig. 1. Scheme illustrating the formation of the anamorphic image of the diffraction plane.

within the system [19]. An anamorphic image represents a stigmatic image which is strongly distorted in first order. For example, a circle will be imaged as an ellipse or a square as a rectangle, as illustrated schematically in Fig. 1. The ratio of the maximum and the minimum diameter defines the distortion D .

The arrangement of the magnetic quadrupoles, the course of their axial strength $\Psi_2 = \Psi_2(z)$, and the course of the fundamental rays $x_\alpha, y_\beta, x_\gamma, y_\delta$ are shown in Fig. 2 for an obstruction-free phase shifter with two orthogonal anamorphic images of the diffraction plane exhibiting a large distortion $D = x_\alpha(z_1)/y_\beta(z_1) = y_\beta(z_2)/x_\alpha(z_2) \approx 125$. The field rays x_γ, y_δ intersect the center of the back-focal plane of the objective lens and the centers z_1 and z_2 of the anamorphic images. Owing to the symmetry of the quadrupole strength $\Psi_2(z)$ and the fundamental rays, the system does not introduce off-axial aberrations. In order to restrict the magnitude of the axial aberrations the value $x_\alpha(z_1) = y_\beta(z)$ of the axial rays at the anamorphic images of the diffraction plane must not exceed significantly the focal length f_0 of the objective lens. We achieve this condition by adjusting the intermediate magnification M appropriately.

The long side of the first anamorphic image at the plane z_1 points in the x -direction, whereas that of the second anamorphic image at the plane z_2 points in the y -direction. We place the cylindrical microphase plate shown in Fig. 3 at the plane z_1 in such a way that its x -axis is centered along the long axis of the anamorphic image. The same phase plate is centered along the y -axis at the plane z_2 . The first phase plate shifts the phase of the scattered wave by $\chi_{p1} = \chi_0/2$ if the x -component of the two-dimensional scattering angle θ lies in the range $\theta_p < |\theta_x| \leq \theta_0$. Accordingly, the phase will not be shifted for scattering angles which are located in the angular stripe $\theta_y, |\theta_x| \leq \theta_p$. The second phase plate shifts the phase by $\chi_{p2} = \chi_0/2$ for scattering angles with y -components in the domain $\theta_p < |\theta_y| \leq \theta_0$. The phase is not shifted for scattering angles located in the angular domain $\theta_x, |\theta_y| \leq \theta_p$. The combined phase shift of the two phase plates is shown in Fig. 4. The figure demonstrates that the total $\chi_p(\theta_x, \theta_y)$ phase

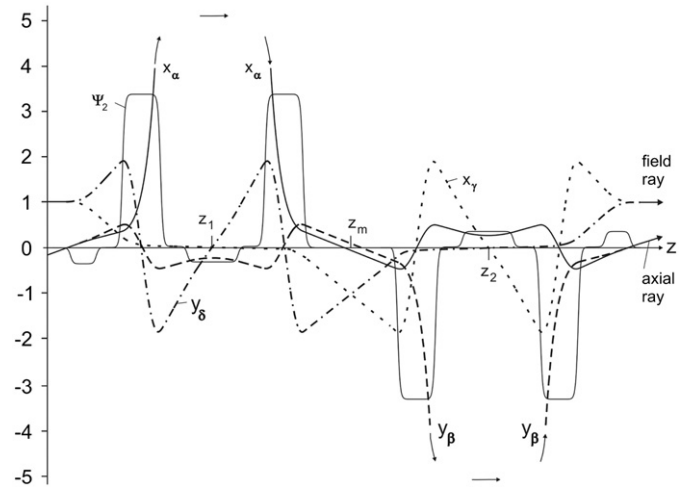


Fig. 2. Course $\Psi_2 = \Psi_2(z)$ of the axial magnetic quadrupole strength and course of the field rays x_γ, y_δ and the axial rays x_α, y_β , respectively, along the optic axis within the phase shifter. Anamorphic images of the diffraction plane are located at the planes z_1 and z_2 where cylindrical phase plates are placed.

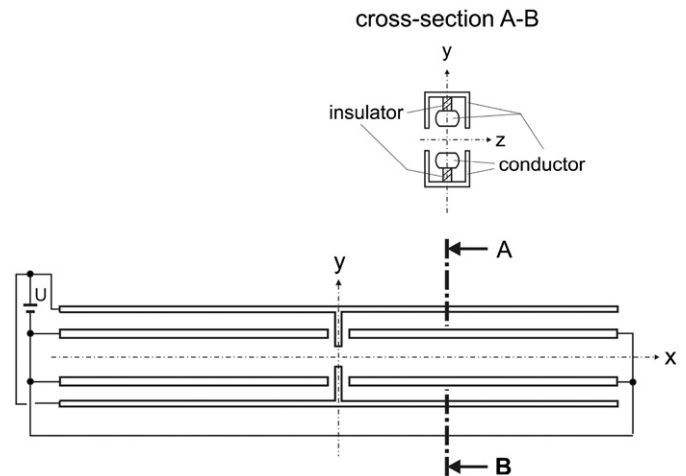


Fig. 3. Scheme of the obstruction-free phase plate centered about the line-shaped anamorphic image of the diffraction plane.

shift closely resembles that of a Zernike phase plate apart from to narrow stripes. Nevertheless, the phase contrast transfer function for these stripes will only be reduced by a factor of 0.71 for $\chi_0 = \pi/2$.

14. Conclusion

The highest attainable specimen resolution is a function of the tolerable dose, the object thickness, the threshold electron energy for atom displacement, the contrast, and the required signal to noise ratio. To maximize this ratio, we must utilize as many scattered electrons as possible. We can largely meet this condition by incorporating an achromatic aplanat and an obstruction-free phase shifter into the TEM whose accelerating voltage can be varied according to the requirements imposed by the object. In order to increase the resolution of radiation-sensitive objects, the instrumental resolution limit and the contrast must be made as large as possible. The highest achievable contrast is negative. It can be obtained by adjusting appropriately the phase shift of the

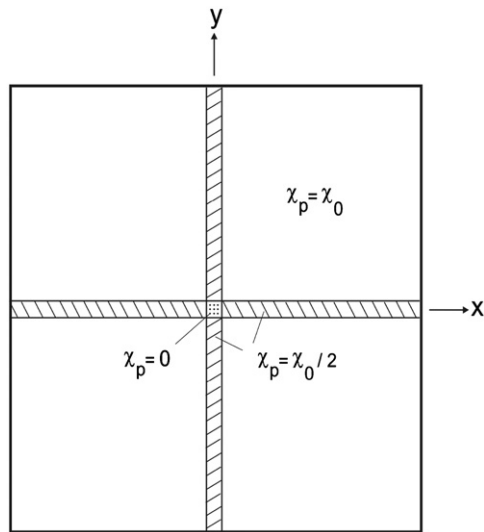


Fig. 4. Total phase shift $\chi_p(x, y)$ of the phase shifter referred back to the diffraction plane.

phase shifter, the defocus and the spherical aberration of the aberration-corrected objective lens. At present, the parasitic electrical and mechanical instabilities pose the main obstacles because they prevent an appreciable reduction of the information limit rather than the residual defects of the aberration-corrected lens system.

Acknowledgements

I want to thank Dr. J. Zach (CEOS) for numerical computation of the paraxial rays shown in Fig. 2 and Professor R. Schroeder (Heidelberg) for placing Fig. 1 at my disposal.

References

- [1] D. Gabor, A new microscope principle, *Nature* 161 (1948) 77.
- [2] E.N. Leith, J. Upatnick, *J. Opt. Soc. Am.* 52 (1962) 1123.
- [3] G. Moellenstedt, H. Dueker, *Z. Phys.* 145 (1956) 377.
- [4] H. Lichte, M. Lehmann, *Rep. Prog. Phys.* 71 (2008) 016102.
- [5] H. Lichte, *Ultramicroscopy* 108 (2008) 256.
- [6] D. Geiger, A. Rother, H. Lichte, M. Linck, D. Wolf, F. Röder, Ch. Matzeck, S. Gemming, I. Chaplygin, *Microsc. Microanal.* 13 (Suppl. 3) (2007) 306.
- [7] K.-H. Hanszen, *Holography in Electron Microscopy*, in: *AEEP* 59 (1982) 1.
- [8] A. Tonomura, *Electron Holography*, Springer, Berlin, 1999.
- [9] O. Scherzer, *Z. Phys.* 101 (1936) 593.
- [10] O. Scherzer, *J. Appl. Phys.* 20 (1949) 20.
- [11] M. Haider, H. Rose, S. Uhlemann, B. Kabius, K. Urban, *J. Electron Microsc.* 47 (1998) 395.
- [12] O. Krivanek, N. Dellby, A.R. Lupini, *Ultramicroscopy* 78 (1999) 1.
- [13] H. Lichte, D. Geiger, M. Haider, B. Freitag, *Proc. Microsc. Microanal.* (2004) 112.
- [14] H. Rose, *Ultramicroscopy* 15 (1984) 173.
- [15] H. Rose, *Image Formation in the Electron Microscope*, lecture script 1989/1990 (in German), available from: info@CEOS-GmbH.de.
- [16] M. Lentzen, *Ultramicroscopy* 99 (2004) 211.
- [17] H. Rosein: F. Ernst, M. Rühle (Eds.), *High-Resolution Imaging and Spectroscopy of Materials*, Springer, Heidelberg, 2003.
- [18] H. Rose, *Ultramicroscopy* 2 (1977) 251.
- [19] R. Schroeder, B. Barton, H. Rose, G. Benner, *Microsc. Microanal.* 13 (Suppl. 3) (2007) 008.